

Cell Injury, Repair, Aging and Apoptosis

Radioprotective Effect of Heat Shock Protein 25 on Submandibular Glands of Rats

Hae-June Lee,* Yoon-Jin Lee,*
Hee-Chung Kwon,[†] Sangwoo Bae,*
Sung-Ho Kim,[‡] Jung-Joon Min,[§] Chul-Koo Cho,[¶]
and Yun-Sil Lee*

From the Laboratories of Radiation Effect* and Molecular Cancer,[†] and the Department of Radiation Oncology,[‡] Korea Institute of Radiological and Medical Sciences, Seoul; and the College of Veterinary Medicine[§] and the Department of Nuclear Medicine,[¶] Chonnam National University, Gwangju, Korea

Irradiation (IR) is a fundamental treatment modality for head and neck malignancies. However, a significant drawback of IR treatment is irreversible damage of salivary gland in the IR field. In the present study, we investigated whether heat shock protein (HSP) 25 could be used as a radioprotective molecule for radiation-induced salivary gland damage in rats. HSP25 as well as inducible HSP70 (HSP70i) that were delivered to the salivary gland via an adenoviral vector significantly ameliorated radiation-induced salivary fluid loss. Radiation-induced apoptosis, caspase-3 activation, and poly(ADP-ribose) polymerase cleavage in acinar cells, granular convoluted cells, and intercalated ductal cells were also inhibited by HSP25 or HSP70i transfer. The alteration of salivary contents, including amylase, protein, Ca⁺, Cl⁻, and Na⁺, was also attenuated by HSP25 transfer. Histological analysis revealed almost no radiation-induced damage in salivary gland when HSP25 was transferred. Aquaporin 5 expression in salivary gland was inhibited by radiation; and HSP25 transfer to salivary gland prevented this alteration. The protective effect of HSP70i on radiation-induced salivary gland damage was less or delayed than that of HSP25. These results indicate that HSP25 is a good candidate molecule to protect salivary gland from the toxicity of IR. (Am J Pathol 2006, 169:1601–1611; DOI: 10.2353/ajpath.2006.060327)

Irradiation (IR) delivery to head and neck is a common treatment modality for malignancies, and the radiation field frequently includes salivary glands. Salivary glands in the IR field are severely damaged, consequently re-

sulting in marked salivary hypofunction in ~80% of patients.^{1–3} Patients experiencing reduced salivary flow suffer from considerable morbidity including dental caries, mucosal infections, dysphagia, and extensive discomfort. Although the effects of IR have been recognized as a significant clinical problem for more than 90 years, the mechanism of these effects remains unknown, and no adequate prevention or treatment is yet available. Saliva is essential for maintaining the health of the oral cavity.⁴ Although salivary glands should be considered to be radioresistant because of their highly differentiated cellular state,⁵ their function is rapidly affected when they are exposed to ionizing radiation.⁶ Serous cells are considered to be more radiosensitive than mucous cells because serous secretory granules are rich in transition metals such as Zn²⁺, Fe²⁺, and Mn²⁺, which may leak into the cytoplasm and cause autolysis and cell death.⁷ At later stages changes in salivary gland and reduction in salivary function are observed within 3 months to 1 year.^{2,3}

Aquaporins (AQPs) are specific water channels that allow rapid transcellular movement of water in response to osmotic/hydrostatic pressure gradients.⁸ AQP5, cloned from submandibular glands, is present in the water-transporting epithelia of lacrimal gland, trachea, eye, lung, and salivary glands of rat.⁹ In human salivary glands, AQP5 is anatomically localized in the apical membranes of acinar cells, but not in those of ductal cells,¹⁰ and functions to stimulate the outflow of water into the acinar lumen. In fact, a reduction of salivary gland secretion has been shown in mice harboring a mutant AQP5 channel.¹¹

Heat shock proteins (HSPs) are a group of highly conserved proteins originally identified as proteins that are up-regulated in response to elevated temperatures; however, they are now shown to be induced by a wide range of noxious or stressful stimuli, including heat, hypoxia,

Supported by the Korea Science and Engineering Foundation and the Ministry of Science and Technology, Korean Government, through the National Nuclear Technology Program.

Accepted for publication July 20, 2006.

Address reprint requests to Yun-Sil Lee, Laboratory of Radiation Effect, Korea Institute of Radiological and Medical Sciences, 215-4 Gongneung-Dong, Nowon-Ku, Seoul 139-706, Korea. E-mail: yslee@kcch.re.kr.

ischemia, and heavy metals.¹²⁻¹⁴ A number of studies have shown that a mild stress induces rapid synthesis of HSP27, -70, and -90, which then confer cells with some protection against further and more severe cellular insult.¹⁵⁻¹⁸ Although it is likely that the various HSPs function in a coordinated manner to protect the cell after stress, overexpression of a single species (HSP27, -70, or -90) can also confer cells with resistance to various stimuli.¹⁹⁻²² HSP25 (or HSP27) has been suggested to protect cells against apoptotic cell death triggered by hyperthermia, ionizing radiation, oxidative stress, Fas ligand, and cytotoxic drugs,^{1-3,23,24} and several mechanisms have been proposed to account for HSP27-mediated apoptotic protection. For example, its specific interaction with cytochrome c released from mitochondria into the cytosol prevents apoptosome formation,^{25,26} and elimination of unfolded protein through extralysosomal, energy-dependent, ubiquitin-proteasome degradation pathway contributes to protection of cells from stressful stimuli.⁷ HSP27 binds to polyubiquitin chains as well as 26S proteasomes, and the ubiquitin-proteasome pathway is involved in the activation of transcription factor nuclear factor (NF)- κ B by degrading its main inhibitor I- κ B α .⁷ Moreover, phosphorylated HSP27 has been shown to bind the adaptor protein Daxx and then to inhibit Fas-mediated apoptosis.⁴ Interaction between HSP27 and Akt is necessary for Akt activation, which is then followed by dissociation of phosphorylated HSP27 from Akt.⁵ We recently reported that the radioprotective effect of HSP25 involves delayed cell growth^{27,28} and HSP25-mediated MnSOD gene expression.^{29,30} HSP25 overexpression down-regulates ERK1/2 expression^{28,30} and also inhibits radiation-induced PKC δ -mediated production of reactive oxygen species and cell death.³¹ However, a radioprotective effecting an *in vivo* system has not yet been evaluated.

The aim of this study was to evaluate the potential of exogenous HSP25 expression, delivered by adenoviral vectors, to protect rats from radiation-induced salivary gland damage. We showed that overexpression of HSP25 in salivary glands could significantly inhibit radiation-induced cell death, saliva fluid loss, and alteration of saliva chemistry and AQP5 expression.

Materials and Methods

Description of the Genes

Mouse cDNAs for HSP25 and inducible HSP70 (HSP70i) were cloned by polymerase chain reaction (PCR) into pGFP3 vector to make pGFP3-HSP25 and pGFP3-HSP70i fusion constructs. Because only the coding sequence was cloned, no flanking sequence was added into the vector. GFP (green fluorescent protein) tag was attached at the C terminus of the HSPs to monitor the efficiency of the protein expression during DNA construction. The following primers were used in PCR to prepare those constructs: for pGFP3-HSP25 cloning, forward primer 5'-CGGAATTCATGACCGAGCGCCGCGTGCCCC-TT-3', reverse primer 5'-CTAGTCTAGATTACTTGGCTC-

CAGACTGTTCA GA-3' and for pGFP3-HSP70i cloning, forward primer 5'-CCGGAATTCGCCAAAGCCGCGGC-GATCGGC-3' and reverse primer 5'-CGCGGATCCATC-TACCTCCTCAATGGTGGGGCC-3'.

Construction of Recombinant Viral Vectors

To make viral vectors that contained mouse HSP25 and HSP70i cDNA, the sequences in pGFP3-HSP25 or pGFP3-HSP70i were removed by digesting the DNA with *Xho*I and *Xba*I. Isolated inserts were ligated to corresponding restriction sites of pShuttleCMV vector to make pShuttleCMV-HSP25 or pShuttleCMV-HSP70i, respectively.³² These constructs were recombined with pAdEasy-1 to make recombinant viral vectors that contained mouse HSP25 or HSP70i, respectively. Expression of HSPs in mouse was detected by using antibody to HSPs. As a control, we used a recombinant adenovirus that expressed luciferase for convenient detection of expression in the cell.³³ The final plasmids were linearized with *Pac*I and transfected into 293A cells³⁴ using *Wet*-Fect-Q transfection reagent (WeiGENE Inc., Daegu, Korea). Recombinant viruses were harvested by viral plaques 7 to 10 days after transfection. For large scale-production, 30 15-cm plates of 293A cells were infected with recombinant viruses. Two days after infection, when a clear CPE was visible, cells were harvested by low-speed centrifugation. The cell pellets resuspended with Dulbecco's modified Eagle's medium were repeatedly frozen at -80°C and thawed in a 37°C water bath for a total of four cycles. The samples were spun at 12,000 rpm for 10 minutes, and viral supernatant was stored at -80°C . The recombinant virus particles were purified by cesium chloride gradient ultracentrifugation.³⁵ Virus titers were determined by tissue culture infectious dose 50 (TCID₅₀). Typical virus titers were 10^9 to 10^{10} pfu/ml.

Reagents

Amifostine [2-(3-aminopropyl)aminoethyl phosphorothioate; WR2721] was obtained from Sigma-Aldrich Co. (St. Louis, MO). A solution of 100 mg/ml was prepared in 0.9% NaCl and stored at 4°C .

Animals

Wistar male rats (250 to 300 g body weight) were purchased from SLC (Hamamatsu, Japan) and kept in polycarbonate cages under an alternating 12-hour light/dark cycle. Animals were maintained at animal care facilities, and food and water were supplied *ad libitum*. Studies were conducted under guidelines for the use and care of laboratory animals and were approved by the Institutional Animal Care and Use Committee of the Korea Institute Radiological and Medical Sciences.

Experimental Design

Rats were divided into nine groups, and each group consisted of three rats. Each animal was treated as de-

scribed. Group I (normal control) received no pretreatment, group II (radiation control) was irradiated only, group III (vector control) was control adenoviral vector transferred, group IV was adenovirus with *HSP25* gene transferred, group V was adenovirus with *HSP70i* gene transferred, group VI was viral vector transferred and irradiated, group VII was *HSP25* gene transferred and irradiated, group VIII was *HSP70i* gene transferred and irradiated, and group IX was pretreated with amifostine (100 mg/kg per body weight, i.v.) and irradiated.

IR of Salivary Glands

All rats were subjected to 17.5 Gy of radiation directed to the submandibular glands. Animals were first anesthetized with a combination of ketamine chloride (6 mg/kg) and xylazine (0.6 mg/kg) injected intraperitoneally. Head and neck regions of animals, including bilateral submandibular glands, were exposed to a single dose of 17.5 Gy at a dose rate of 190 cGy/minute. Size of the IR field was controlled (Theratron 780; AECL, Ontario, ON, Canada), and the radiation field was 4 × 34 cm and an 80-cm source-to-skin distance. Radiation was given to six rats at a time with ventral surface being exposed to the source. Control animals were sham-irradiated; ie, anesthetized and placed in the irradiator.

In Vivo Gene Transfer to Submandibular Glands

Adenoviral vectors were suspended in Dulbecco's modified Eagle's medium media and delivered to both submandibular glands by direct injection. Individual rats were randomly assigned to receive either control adenoviral vector or adenovirus with *HSP25* or *HSP70i* gene (1×10^8 pfu/gland). All gene transfers were performed 1 day before 17.5-Gy IR. Animals were first anesthetized and 0.5 cm of neck ventral skin was incised. Viral vector was directly injected by a syringe, and the incision was then sutured with silk. Animals received 1 mg of dexamethasone (intramuscularly) at the time of gene transfer to suppress inflammation due to adenoviral infection. On the following day after gene transfer, distribution of viral vector was monitored with an IVIS ImagingSystem (Xenogen, Alameda, CA).

Collection of Saliva and Harvesting of Salivary Glands

Forty and 90 days after IR, animals were weighed and then anesthetized with a combination of ketamine and xylazine. Saliva flow rates were measured for both right and left submandibular gland of each rat. The orifices of main excretory duct of the submandibular glands were identified intraorally and cannulated with polyethylene tubing (PE-10; Becton Dickinson and Company, Mountain View, CA). The total saliva was collected for 30 minutes after subscapular injection with pilocarpine hydrochloride (Sigma-Aldrich Inc., Steinheim, Germany). Saliva flow rates were expressed as the volume of saliva

secreted per 100 g of body weight. Submandibular glands were harvested immediately after saliva collection and weighed after carefully trimming fat and connective tissue. Body and gland weights were obtained for all animals in which flow measurements were performed.

Sialochemical Analysis

Salivary constituents of the submandibular glands were analyzed. Concentrations of sodium, potassium, chloride, and total protein were determined with a Hitachi Clinical Analyzer 7180 (Hitachi High-Technologies Co., Tokyo, Japan), and ionized calcium was measured with AVL 9180 (Diamond Diagnostics, Holliston, MA). Amylase was determined with Fuji DRI Chemclinical Chemistry Analyzer 3500 (Fuji Photo Film Co., Tokyo, Japan).

Immunohistochemistry and Light Microscopic Examination

The rat submandibular glands were removed, postfixed for 1 hour in the same fixative solution using perfusion, dehydrated in ethanol followed by xylene, and then finally embedded in paraffin. Sections were cut at 3- μ m thickness on a rotary microtome (Leica, Wetzlar, Germany), dewaxed, and then rehydrated. For immunoperoxidase labeling, endogenous peroxidase was blocked by 0.3% H₂O₂ in absolute methanol for 15 minutes at room temperature. For antigen retrieval, sections were placed in citrate buffer (pH 6.0) and heated in a microwave oven for 10 minutes. Nonspecific binding for immunoglobulin was prevented by incubating the sections in blocking solution (Cap-Plus detection kit; Zymed Laboratories, San Francisco, CA) for 20 minutes. Sections were incubated overnight at 4°C with primary antibody diluted in antibody diluent (Zymed Laboratories), followed by three washes (5 minutes each) with phosphate-buffered saline (PBS) containing 0.05% Triton X-100. Incubation with corresponding secondary antibody and the peroxidase-antiperoxidase complex was performed for 30 minutes at 22°C. Immunoreactive sites were visualized using 3,3'-diaminobenzidine 0.1% (w/v) and 0.03% (v/v) hydrogen peroxide solution.

Antibodies and Chemicals

The following primary antibodies were used: goat-polyclonal IgG HSP25 (M-20; Santa Cruz Biotechnology, Santa Cruz, CA), goat-polyclonal IgG AQP5 (C-19, Santa Cruz Biotechnology), mouse monoclonal anti-HSP70 (SPA-810; Stressgen Biotechniques Inc., San Diego, CA), mouse monoclonal anti-proliferating cell nuclear antigen (PC-10; DAKO, Kyoto, Japan), anti-cleaved-caspase3 (Asp175) (5A1; Cell Signaling Technology Inc., Beverly, MA), and anti-poly(ADP-ribose) polymerase (PARP) (no. 9542; Cell Signaling Technology Inc.) antibodies. Anti-mouse and anti-rabbit secondary antibodies and the corresponding peroxidase-anti-peroxidase complexes used were from Cap-Plus detection kit (Zymed). Anti-goat sec-

ondary antibody was N-His-tofine Simple Stain MAX PO, Universal Immuno-Peroxidase Polymer (anti-goat), H0502 (Nicheirei Bioscience Inc., Kyoto, Japan). Triton X-100, hydrogen peroxide, PBS, and other chemicals were purchased from Sigma-Aldrich Co. (St. Louis, MO).

Terminal dUTP Nick-End Labeling (TUNEL) Assay

Apoptotic cells in salivary gland were visualized, using the In Situ Cell Death Detection kit (Roche Diagnostic GmbH, Mannheim, Germany), by the indirect TUNEL method following the manufacturer's protocol. The paraffin-embedded tissue sections were hydrated and incubated with the TUNEL reaction mixture containing TdT and fluorescein-dUTP without proteinase K pretreatment. The reactions were terminated by three washes with PBS. Anti-fluorescein-peroxidase antibody was applied, and the reaction was visualized by 3,3'-diaminobenzidine. Sections were counterstained with autohematoxylin. Negative control sections were incubated with distilled water in the absence of TdT.

Immunoblotting

Whole submandibular gland sections (~1 mm thick) were homogenized with a PRO200 homogenizer (PROScientific, Oxford, UK) in lysis buffer (PRO-PREP, Sungnam, Korea). The protein concentration was determined by the Bradford method (Bio-Rad, Richmond, CA). For polyacrylamide gel electrophoresis and Western blot, proteins were solubilized with lysis buffer [120 mmol/L NaCl, 40 mmol/L Tris (pH 8.0), and 0.1% Nonidet P-40], the samples were boiled for 5 minutes, and equal amounts of protein (80 µg/well) were analyzed on 10% sodium dodecyl sulfate-polyacrylamide gel electrophoresis. After electrophoresis, proteins were transferred onto a nitrocellulose membrane and processed for immunoblotting. Blocking was performed by incubation with 5% nonfat dry milk in PBS-0.1% Tween 20 (PBS-T) for 2 hours at room temperature. After blocking, membranes were probed with the corresponding antibody for 18 hours at 4°C and washed with PBS-T. Blots were further incubated with horseradish peroxidase-conjugated secondary antibody, diluted at 1:5000, and specific bands were visualized by enhanced chemiluminescence (Amersham International, Buckinghamshire, UK). Autoradiographs were recorded onto X-Omat duplicating films (Eastman Kodak Co., Rochester, NY).

Quantification

For the quantification of TUNEL-positive signals, five sections were randomly chosen for each animal. In each section, ~500 acinar cells, granular convoluted cells, and intercalated ductal cells were randomly counted at a magnification of 400, and the percentage of TUNEL-positive cells was calculated. For the quantification of HSP25 or HSP70i expression, we randomly chose five

fields of each slide (three slides in each group) and took pictures using microscopy with digital camera (Leica DM IRBE; Leica Microsystems GmbH). The positive signals were measured by image analyzing software (Leica QWin) in the same area of each field; field size was 200 × 200 µm at a magnification of ×200. Percentage of positive signal was obtained in the unit area of submandibular gland, and the results were compared on days 1 (after gene transfer), 40, and 90 (after IR). For the detection of AQP5 expression, we used similar methods for HSP25 or HSP70i, but the field size was 60 × 50 µm and the numbers of fields were 10 in each slide at ×1000 magnification. We obtained positive signal ratio of AQP5 against normal control at 40 and 90 days after IR. The labeling incidences of each animal were obtained by averaging the percentages of sections or fields, and then mean and SD were determined at each time point for three experimental animals. Comparison between experimental and control data at each time point was made by one-way analysis of variance followed by the Student's *t*-test, with *P* < 0.05 as statistically significant.

Results

Transfer of HSP25 and HSP70i to Rat Submandibular Gland Using Adenoviral Vector System

The distribution of virus after transfer of *HSP25* to submandibular gland was first investigated, using a virus encoding firefly luciferase (Fluc) that was administered at a titer equivalent to that used for *HSP25*-expressing viruses (1×10^8 pfu/ml). Bioluminescence imaging for luciferase was performed by image analyzer on the next day after the transfer, and active luminescence was detected in submandibular glands (Figure 1A), indicating that localization of transferred virus was the submandibular glands. Immunohistochemical analysis revealed that *HSP25* was overexpressed mainly in acinar cells, whereas *HSP70i* was in granular convoluted cells. Some *HSP70i* was expressed also in ductal cells. As seen in Figure 1B, in irradiated submandibular glands, radiation induced loss of *HSP25* and *HSP70i* at 40 and 90 days; however, *HSP25*-transferred glands were found to have more *HSP25* protein than other groups. It should also be noted that radiation induced a slight reduction of endogenous *HSP25* or *HSP70i* in irradiated normal control group, and this was probably attributable to radiation-induced death of some cells containing HSPs. There were no differences detected between irradiated and nonirradiated control rats. In the case of amifostine-treated rats, no induction of *HSP25* or *HSP70i* was detected (Figure 1, B and C).

Effects on Radiation-Induced Glandular Weight Loss

When body weights were compared at 40 and 90 days after radiation, 17.5-Gy radiation was found to signifi-

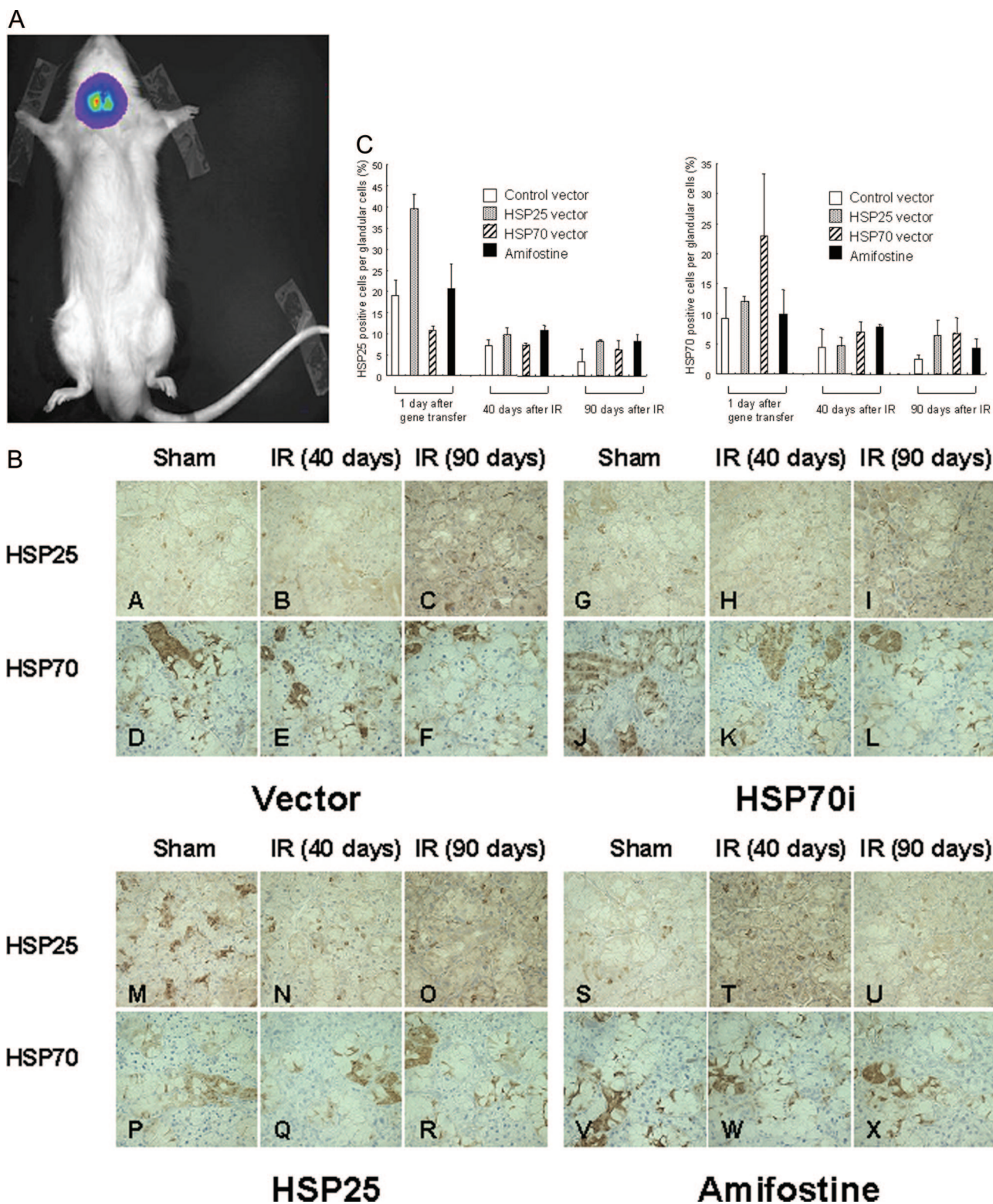


Figure 1. Bioluminescence imaging (BLI) and immunolocalization of HSP25 and HSP70i in *HSP25* and *HSP70i* transferred rat. **A:** BLI of luciferase expression in a living rat at 24 hours after gene transfer into salivary gland. Active luminescence was detected in bilateral submandibular glands of the rat. **B:** Expression of HSP25 and HSP70i during the days after IR. Representative photographs show expression changes of HSP25 and HSP70i in rats after transfer of control adenoviral vector (**A–F**) and HSP70i-expressing (**G–L**) and HSP25-expressing (**M–R**) adenovirus and pretreatment with amifostine (**S–X**). HSP25 was expressed in acinar cells and HSP70i in granular convoluted cells. **C:** Distributions of HSP25 and HSP70i during experimental periods. The graphs indicate the percentage (mean \pm SD) of HSP25- or HSP70i-positive cells against the unit area ($200 \times 200 \mu\text{m}^2$, $\times 200$) of submandibular gland at 24 hours after gene transfer and 40 and 90 days after 17.5 Gy IR using image analyzer. Each group consisted of three rats, and five fields were obtained from each animal. Original magnifications, $\times 200$.

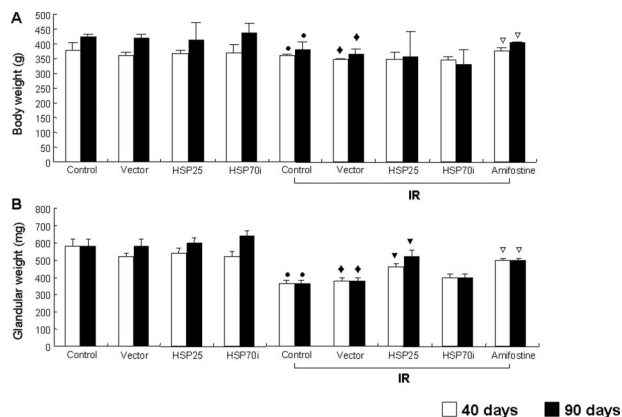


Figure 2. Total body weight and submandibular gland weight of rats. Measurements were obtained 40 and 90 days after 17.5-Gy IR of head and neck. **A:** Changes of total body weight during experimental periods. Radiation significantly reduced body weight of animals, and amifostine significantly prevented the loss of body weight induced by IR. **B:** The weights of submandibular glands. HSP25 and amifostine significantly attenuated the loss of glandular weight compared with each controls. Differences of body weight and glandular weight, compared with controls, are indicated by ●, compared with normal control; ◆, compared with vector transferred control; ▼, compared with vector transferred IR control; and ▽, compared with radiation control ($P < 0.05$).

cantly reduce body weights, and *HSP25* and *HSP70i* transfer could not prevent radiation-induced body weight loss. When treated with amifostine, which has radioprotective effects and has been approved by the United States Food and Drug Administration, the loss of body weight by radiation was significantly prevented compared with the level of nonirradiated control rats (Figure 2A). Glandular weights were also decreased by radiation; however, the decrease was significantly attenuated when *HSP25* was transferred to submandibular glands. Amifostine treatment 30 minutes before radiation restored the glandular weights inhibited (Figure 2B). On the other hand, *HSP70i* did not show any protection from radiation-induced glandular weight loss. These results indicate that *HSP25* protected the animal from the radiation-induced loss of glandular weight.

Effects on Pilocarpine-Stimulated Saliva Flow Rate and Chemistry

Salivary secretion, represented as salivary flow rate ($\mu\text{l}/30$ minutes/ 100 g body weight), was significantly reduced by radiation compared with nonirradiated control rats. Transfer of control vector alone also affected salivary flow rate, when examined at 90 days of virus transfer. Combined treatment of *HSP25*, *HSP70i*, or amifostine with radiation significantly ameliorated the damage of salivary flow rate (Table 1), when examined 40 and 90 days after IR. Chemical constituents of saliva such as amylase, total protein, Ca^{2+} , Na^{+} , and Cl^{-} , were decreased by radiation, whereas the content of K^{+} was increased by radiation and lasted for 90 days after radiation. Transfer of *HSP25* before IR significantly inhibited these radiation effects; however, no effect was observed by *HSP25* on the K^{+} content. The effect of *HSP25* was much stronger at 40 days after radiation than 90 days.

Table 1. Salivary Flow Rate Stimulated by Pilocarpine of the Different Groups of Rats

Groups	Salivary flow rate ($\mu\text{l}/30$ minutes/ 100 g body weight)	
	40 days	90 days
Normal control	20.99 ± 2.18	21.35 ± 3.15
Vector control	21.40 ± 5.03	$17.2 \pm 1.13^*$
<i>HSP25</i>	17.63 ± 5.69	21.73 ± 10.3
<i>HSP70i</i>	23.07 ± 3.04	15.56 ± 11.77
Irradiation control	9.97 ± 2.28	$5.19 \pm 3.53^*$
Vector + IR	$7.27 \pm 0.75^\dagger$	$6.61 \pm 4.70^\dagger$
<i>HSP25</i> + IR	$15.21 \pm 4.03^\ddagger$	$15.21 \pm 4.03^\ddagger$
<i>HSP70i</i> + IR	$12.04 \pm 4.99^\ddagger$	$12.58 \pm 2.59^\ddagger$
Amifostine + IR	$13.65 \pm 0.61^\S$	$16.39 \pm 3.42^\S$

Values are mean \pm SD of three rats per groups.

*Significantly different from the normal control group.

†Significantly different from the vector control group.

‡Significantly different from the vector-transferred irradiation control group.

§Significantly different from the irradiation control group.

*†‡§Statistical significance of $P < 0.05$.

HSP70i transfer showed protective effect only on the content of protein at 40 days of radiation, but amifostine showed protective effect on all salivary constituents examined until 90 days of radiation (Table 2).

Histopathology of Submandibular Gland

Histopathological analysis revealed vacuolization of acinar cells and pyknotic nuclei in irradiated rats at 40 days of radiation. These findings were more apparent at 90 days of radiation, when strong vacuolization of almost all acinar cells, many pyknotic nuclei, and lysis of acini were observed. However, transfer of *HSP25* or *HSP70i* genes to submandibular gland and treatment with amifostine diminished vacuolization of acinar cells and pyknotic nuclei; the lobular structure and the cell membranes appeared to be remarkably normal, and the duct system was also relatively unaffected. Further, radiation-induced fibrosis in periductal connective tissue was decreased by *HSP25* or *HSP70i* transfer and amifostine treatment. A similar protective effect was observed among the groups treated with *HSP25*, *HSP70i*, or amifostine. Treatment with viral vector alone did not affect histology of submandibular gland, and transfer of *HSP25* or *HSP70i* alone did not affect either (Figure 3).

Apoptosis of Submandibular Gland

In all gland compartments such as acinar cells, granular convoluted cells, and intercalated ductal cells, apoptotic activity was seen to increase with radiation, when TUNEL assay was performed at 1, 40, and 90 days after radiation. Peak induction of apoptosis was observed at 1 day after radiation and was found to decrease at 40 and 90 days of radiation. Vector control-transferred rats showed more apoptosis by radiation than that of the irradiated normal control group. Transfer of *HSP25* or *HSP70i* to submandibular gland before IR significantly reduced radiation-induced apoptosis, and the degree of reduction was higher in acinar cells than granular convoluted cells

Table 2. Sialochemistry at 40 and 90 Days after Irradiation

Groups	Amylase (U/L)	Protein (g/L)	Ca ⁺ (mmol/L)	Cl ⁻ (mmol/L)	K ⁺ (mmol/L)	Na ⁺
Normal control	62,650 ± 15,450	9.66 ± 5.03	0.35 ± 0.10	37.67 ± 0.28	42.6 ± 2.95	37.33 ± 0.58
40 days						
Vector control	93,786 ± 20,616*	11.33 ± 0.58	0.56 ± 0.05	38.00 ± 3.46	39.70 ± 1.11	38.33 ± 4.16
HSP25	70,613 ± 10,394*	13.00 ± 2.65	0.60 ± 0.08	44.67 ± 5.03	44.27 ± 2.53*	41.33 ± 5.86
HSP70i	45,920 ± 5619*	13.33 ± 2.89	0.72 ± 0.17	51.00 ± 8.72*	40.13 ± 4.36	53.33 ± 9.24
Irradiation control	53,568 ± 6670*	12.20 ± 3.27	0.45 ± 0.10	33.00 ± 5.29	42.68 ± 4.63	29.40 ± 5.55
Vector + IR	26,826 ± 12,962 [†]	7.33 ± 1.53 [†]	0.31 ± 0.13 [†]	31.0 ± 10.44 [†]	61.27 ± 5.99 [†]	21.33 ± 9.24 [†]
HSP25 + IR	72,320 ± 12,979 [‡]	13.67 ± 1.53 [‡]	0.39 ± 0.09	34.33 ± 4.04	54.23 ± 4.81	28.67 ± 7.23
HSP70i + IR	10,506 ± 743	13.33 ± 2.89	0.25 ± 0.04	27.0 ± 11.36 [‡]	54.20 ± 6.94	19.00 ± 5.00
Amifostine + IR	67,066 ± 472 [§]	13.00 ± 3.00	0.44 ± 0.07	40.67 ± 1.15	48.53 ± 3.17	33.33 ± 3.51
90 days						
Vector control	108,366 ± 9026*	36.0 ± 14.0	0.58 ± 0.04	49.00 ± 1.16	40.60 ± 2.55	47.67 ± 3.40
HSP25	58,333 ± 26,383	52.33 ± 20.9	0.44 ± 0.12	40.67 ± 4.03	44.97 ± 6.32	35.67 ± 9.81
HSP70i	78,633 ± 10,300	30.00 ± 8.52	0.59 ± 0.07	45.67 ± 3.30	44.67 ± 2.36	44.67 ± 2.36
Irradiation control	43,433 ± 30,890*	35.7 ± 19.4	0.06 ± 0.40*	44.0 ± 14.0	53.0 ± 5.00	30.41 ± 0.41
Vector + IR	38,100 ± 12,000 [†]	35.67 ± 19.4	0.32 ± 0.07 [†]	39.33 ± 7.13	50.73 ± 1.33 [†]	33.67 ± 7.85 [†]
HSP25 + IR	67,500 ± 27,168	53.00 ± 28.3	0.43 ± 0.02	42.67 ± 11.95	48.31 ± 5.30	33.73 ± 15.17
HSP70i + IR	33,133 ± 22,931	30.00 ± 8.52	0.31 ± 0.00	39.33 ± 14.1	54.60 ± 5.48	31.00 ± 11.5
Amifostine + IR	87,900 ± 8488 [§]	17.50 ± 2.16 [§]	0.61 ± 0.11 [§]	55.00 ± 4.99	48.60 ± 3.46	49.00 ± 2.45 [§]

Values are mean ± SD of three rats per group.
 *Significantly different from the normal control group.
[†]Significantly different from the vector control group.
[‡]Significantly different from the vector-transferred irradiation control group.
[§]Significantly different from the irradiation control group.
^{††§}Statistical significance of *P* < 0.05.

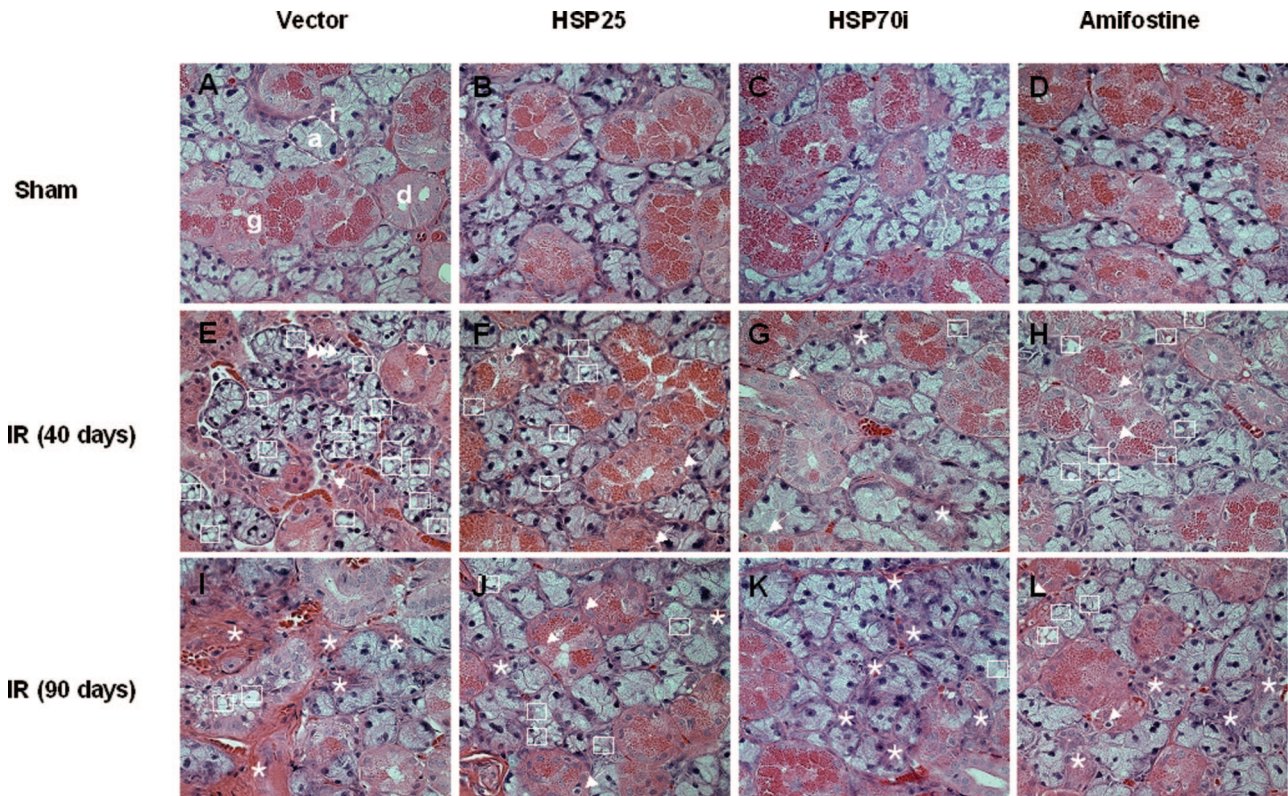


Figure 3. Histopathological analysis of parenchymal changes in damaged salivary gland by radiation. H&E staining of nonirradiated control (A–D), 40 days (E–H) and 90 days (I–L) after 17.5-Gy IR. Nonirradiated control groups are composed of acinar (a), intercalated duct (i), granular convoluted duct (g), and secretory duct (d). At 40 days after 17.5-Gy IR in the vector control group, severe vacuolization (squares), some pyknotic nuclei (arrows), and lysis of acinar or granular convoluted ducts (l) are seen. At 90 days after IR, most of the parenchymal structures in the vector control group are destroyed, with severe fibrosis and some inflammatory infiltration. During the days after IR, HSP25 (F, J), HSP70i (G, K), and amifostine (H, L)-pretreated salivary glands show clearer lobular structures, more acinar and granular convoluted cells, and fewer vacuoles than vector-transferred IR control (E and I). It was more severe at 90 days than at 40 days after IR. Original magnifications, ×400.

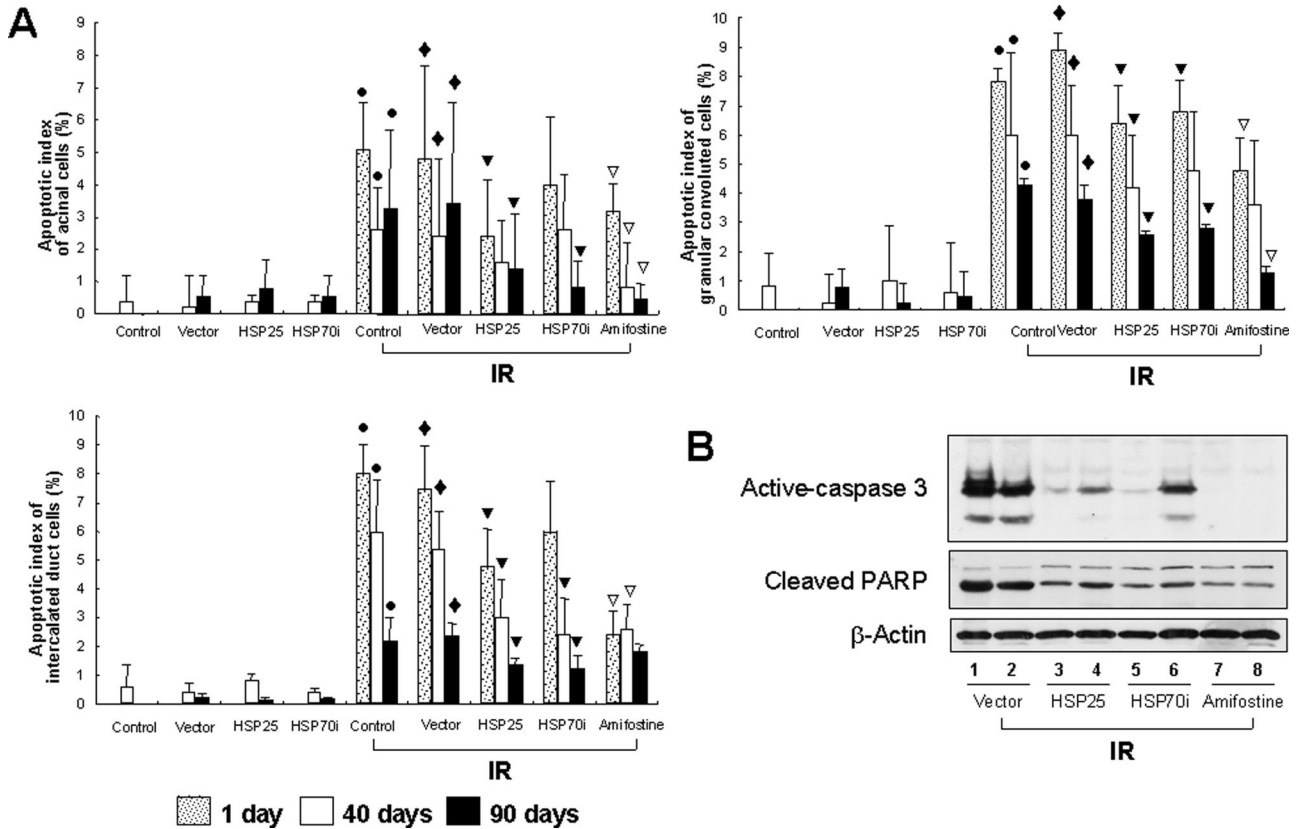


Figure 4. Quantitative analysis of apoptotic cell, active caspase-3, and cleaved PARP. **A:** Apoptotic index of different cell types (mean \pm SD) in control and irradiated submandibular gland at 1 day, 40 days, and 90 days after IR. ●, compared with normal control; ◆, compared with vector transferred control; ▼, compared with radiation control denote statistical significance of $P < 0.05$. **B:** Immunoblot of active caspase-3 and cleaved PARP in damaged submandibular gland at 1 day after 17.5-Gy IR. Activation of caspase-3 and PARP by radiation was inhibited in HSP25-, HSP70i-, and amifostine-pretreated salivary gland. Representative image of two independent animals from each group is shown.

and intercalated ductal cells. In addition, the effect of HSP25 was more evident than HSP70i. When treated with amifostine, effects similar to HSP25-transferred rats were found, but to a lesser extent (Figure 4A). Rats treated with viral vector, HSP25, or HSP70i alone without radiation did not induce any TUNEL-positive cells. Western blotting revealed that rats treated with HSP25 and HSP70i as well as amifostine dramatically reduced radiation-induced cleavage of caspase-3 and PARP when detected at 1 day after radiation (Figure 4B).

AQP5 Expression in Submandibular Gland

AQP5 is topographically localized in the apical membranes of acinar cells and stimulates the outflow of water into the acinar lumen. As seen in Figure 5, AQP5 was well expressed at apical and lateral sides of the plasma membrane without radiation, and treatment with HSP25, HSP70i, and amifostine alone did not affect AQP5 expression. Radiation of 17.5 Gy significantly reduced these expressions from 40 days of radiation, and almost no AQP5 was present at 90 days. However, HSP25 or HSP70i transfer dramatically inhibited AQP5 reduction. The effect of HSP25 was a peak at 40 days of radiation, and the effect of HSP70i was more dominant at 90 days than at 40 days after IR. Amifostine treatment also pre-

vented radiation-induced reduction of AQP5 expression (Figure 5).

Discussion

Because salivary glands are frequently included in the radiotherapy field for the treatment of head and neck malignancies, their function is rapidly impaired.^{36,37} Using a rat model in this study, we showed that HSP25 and HSP70i protected radiation-induced submandibular damage and that this protective effect was attributable to inhibition of cell death and restoration of saliva fluid.

HSP25 (or HSP27) has been suggested to protect cells against apoptotic cell death triggered by heat, ionizing radiation, oxidative stress, Fas ligand, and cytotoxic drugs.^{1-3,23,24} To evaluate the potential of exogenous HSP25 expression, as delivered by adenoviral vectors, a rat salivary gland model with overexpression of HSP25 was used. The histopathological manifestation of radiation damage in the exposed areas of the gland starts relatively late, and no early loss of cells is shown in the major salivary gland. However, early impairment of cellular function (reduction in saliva flow) has been observed and attributed to radiation-induced distortion of signal transduction in the plasma membrane of the secretory

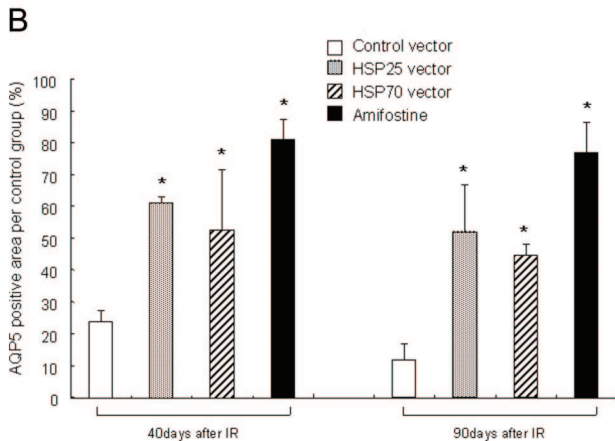
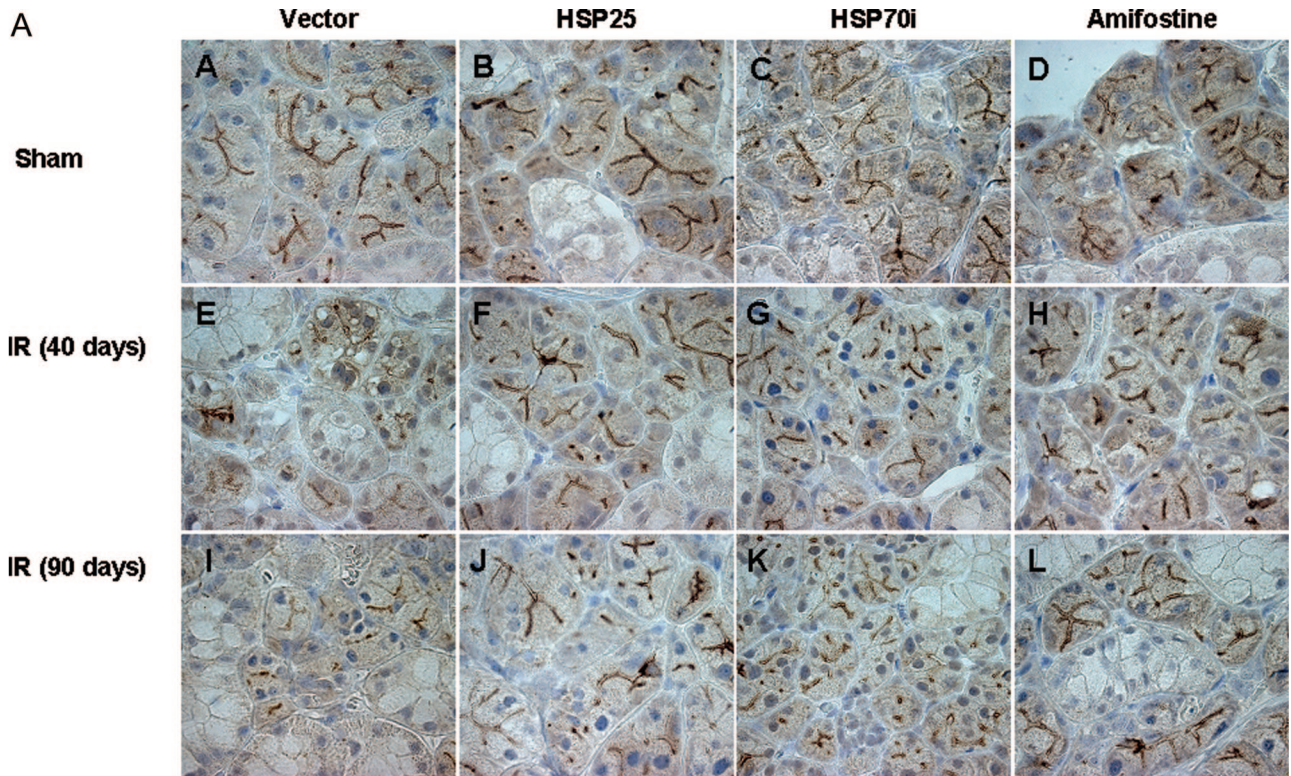


Figure 5. Immunolocalization of AQP5 in irradiated rat salivary gland. **A:** Immunohistochemical analysis for AQP5 was performed at 40 and 90 days after IR. Nuclei were counterstained with autohematoxylin. **A–D:** AQP5 is located at apical membrane of secretory cells, and AQP5-positive cells are abundant in nonirradiated salivary glands. **E and I:** In vector transferred IR control, most of AQP5 activity has disappeared. **J:** HSP25-transferred submandibular glands have AQP5-positive cells until 90 days after IR. **B:** Distribution of AQP5 in salivary gland at 40 and 90 days after IR. The graph indicates the positive signal ratio of AQP5 against normal submandibular gland. There were 10 fields ($60 \times 50 \mu\text{m}^2$, $\times 1000$) per rat in each group. *Significance compared with control group ($P < 0.05$). Original magnifications, $\times 1000$.

cells. In the present study, gene transfer of HSP25 and HSP70i was shown to dramatically prevent radiation-induced damage in the submandibular region. Also, strong vacuolization of acinar cells, many pyknotic nuclei, and lysis of acini by radiation were ameliorated by the transfer of *HSP25* or *HSP70i*, whereas the lobular structure and the cell membranes remained remarkably unchanged, and the duct system was also relatively unaffected by these molecules. Radiation-induced fibrosis in periductal connective tissue was decreased by HSP25 or HSP70i transfer (Figure 3). To elucidate the mechanisms of this protection, induction of apoptosis was examined. Transfer of *HSP25* or *HSP70i* to the submandibular region dramatically reduced radiation-induced apoptosis of acinar cells, granular convoluted cells, and intercalated ductal cells, and reduction of apoptosis by HSP25 or HSP70i was more robust in acinar cells, suggesting spe-

cific protective effect of these molecules on proliferating cells. In fact, cleavages of capase-3 and PARP in submandibular tissue was dramatically reduced by these molecules (Figure 4). These data showed that HSP25 and HSP70i have a protective effect on radiation-induced submandibular gland damage and that its mechanism involves direct inhibition of radiation-induced apoptosis, especially inhibition of apoptosis of proliferating acinar cells. When proliferating cell nuclear antigen-positive cells were examined by immunohistochemistry, no evidence of increased proliferation by HSP25 or HSP70i was seen (data not shown), indicating that HSP25 and HSP70i did not affect cell proliferation but inhibited radiation-induced apoptosis.

Salivary glands of rat are quite similar to human salivary glands in which salivary flow is rapidly reduced after IR.³⁸ Fluid transport in salivary glands is thought to be

osmotically driven in response to transepithelial salt gradients that are generated by ion transport systems localized in the apical and basolateral membranes of the secretory cells. According to the classical two-stage hypothesis,^{39,40} a primary fluid containing plasma-like electrolyte concentrate is generated by the acinar cells, and the fluid is subsequently modified by solute reabsorption and secretion as it passes along the ductal system, resulting in the final hypotonic solution that enters the oral cavity. Therefore, the principal site of water transport is likely to be the acini with relatively little transepithelial water movement occurring in the ducts. Serous cells are considered to be more radiosensitive than mucous cells because serous secretory granules are rich in transition metals such as Zn^{2+} , Fe^{2+} , and Mn^{2+} , which may leak into the cytoplasm, causing autolysis and cell death.⁷ In the present study, changes in salivary function were observed at later stages, such as 40 and 90 days after radiation; however, *HSP25* or *HSP70i* transfer before radiation helped maintain the saliva flow rate and saliva chemistry. *HSP25* transfer maintained amylase, total protein, Ca^{2+} , Na^+ , and Cl^- contents at the level of nonirradiated control rats, suggesting that *HSP25* also affects quality of saliva content. Total salivary protein levels were much higher in all of the groups at 90 days of IR because of increased body weights (1.5- or 2-fold increase of body weight at 90 days when compared with that of the beginning of experiment). We do not know exactly why *HSP70i* could not protect saliva chemistry; only protein content was protected by *HSP70i* at 40 days of radiation. Because protective tendency in other factors such as content of amylase, Ca^{2+} , Cl^- , and Na^+ was not observed by *HSP70i* (Table 2), protective potency of salivary gland appears to be stronger in *HSP25*-transfected cells than in *HSP70i*-transfected cells.

AQP water channels are expressed in a variety of fluid-transporting epithelia, and it is increasingly clear that they are likely to play a significant role in salivary secretion. Several rat exocrine glands have been shown to express AQP5 at the luminal surface of the acinar cells, and they include the lacrimal glands,^{41,42} the subepithelial glands of the upper airways, and the submandibular and parotid salivary glands. AQP5 is highly expressed in the apical plasma membrane,⁴³ and it is suggested to play a significant role in saliva production on the basis of abundance of the channel. Furthermore, knockout mice lacking AQP5 show markedly depressed rates of salivary secretion.^{11,44} AQP5 is abundant in the apical domains of the serous acinar cells, secretory canaliculi, and intercalated ductal cells of rats but absent in the mucous acinar cells and striated duct cells.^{45,46} In our experiment, AQP5 expression was not diminished by radiation when *HSP25* or *HSP70i* was transferred before radiation, suggesting that the protection of acinar cells by these proteins might also involve AQP5 expression (Figure 5).

In conclusion, using a rat model of radiation-induced salivary hypofunction, we show that the transfer of *HSP25* or *HSP70i* protects salivary gland from radiation. Protective effect of *HSP25* was more predominant than *HSP70i* and was similar to the treatment of amifostine, which has been recently approved for use in prevention of xerosto-

mia in head and neck cancer patients undergoing radiotherapy.^{23,24} However, controversy remains as to whether amifostine also confers tumor protection.^{25,26} Therefore, *HSP25* may be a useful target for radiation protection, especially as an adjuvant to radiotherapy of head and neck tumors.

References

1. Grdina DJ, Murley JS, Kataoka Y: Radioprotectants: current status and new directions. *Oncology* 2002, 63(Suppl 2):2-10
2. Nagler RM, Baum BJ: Prophylactic treatment reduces the severity of xerostomia following radiation therapy for oral cavity cancer. *Arch Otolaryngol Head Neck Surg* 2003, 129:247-250
3. Vissink A, Jansma J, Spijkervet FK, Burlage FR, Coppes RP: Oral sequelae of head and neck radiotherapy. *Crit Rev Oral Biol Med* 2003, 14:199-212
4. Takagi K, Yamaguchi K, Sakurai T, Asari T, Hashimoto K, Terakawa S: Secretion of saliva in X-irradiated rat submandibular glands. *Radiat Res* 2003, 159:351-360
5. Coppes RP, Zeilstra LJ, Vissink A, Konings AW: Sialogogue-related radioprotection of salivary gland function: the degranulation concept revisited. *Radiat Res* 1997, 148:240-247
6. Nagler RM: Short- and long-term functional vs morphometrical salivary effects of irradiation in a rodent model. *Anticancer Res* 1998, 18:315-320
7. Abok K, Brunk U, Jung B, Ericsson J: Morphologic and histochemical studies on the differing radiosensitivity of ductular and acinar cells of the rat submandibular gland. *Virchows Arch B Cell Pathol Incl Mol Pathol* 1984, 45:443-460
8. King LS, Yasui M: Aquaporins and disease: lessons from mice to humans. *Trends Endocrinol Metab* 2002, 13:355-360
9. Raina S, Preston GM, Guggino WB, Agre P: Molecular cloning and characterization of an aquaporin cDNA from salivary, lacrimal, and respiratory tissues. *J Biol Chem* 1995, 270:1908-1912
10. Agre P, Brown D, Nielsen S: Aquaporin water channels: unanswered questions and unresolved controversies. *Curr Opin Cell Biol* 1995, 7:472-483
11. Ma T, Song Y, Gillespie A, Carlson EJ, Epstein CJ, Verkman AS: Defective secretion of saliva in transgenic mice lacking aquaporin-5 water channels. *J Biol Chem* 1999, 274:20071-20074
12. Feder ME, Hofmann GE: Heat-shock proteins, molecular chaperones, and the stress response: evolutionary and ecological physiology. *Annu Rev Physiol* 1999, 61:243-282
13. Ehrnsperger M, Gaestel M, Buchner J: Analysis of chaperone properties of small Hsp's. *Methods Mol Biol* 2000, 99:421-429
14. Benjamin IJ, McMillan DR: Stress (heat shock) proteins: molecular chaperones in cardiovascular biology and disease. *Circ Res* 1998, 83:117-132
15. Amin V, Cumming DV, Coffin RS, Latchman DS: The degree of protection provided to neuronal cells by a pre-conditioning stress correlates with the amount of heat shock protein 70 it induces and not with the similarity of the subsequent stress. *Neurosci Lett* 1995, 200:85-88
16. Mailhos C, Howard MK, Latchman DS: Heat shock proteins hsp90 and hsp70 protect neuronal cells from thermal stress but not from programmed cell death. *J Neurochem* 1994, 63:1787-1795
17. Mosser DD, Martin LH: Induced thermotolerance to apoptosis in a human T lymphocyte cell line. *J Cell Physiol* 1992, 151:561-570
18. Samali A, Cotter TG: Heat shock proteins increase resistance to apoptosis. *Exp Cell Res* 1996, 223:163-170
19. Amin V, Cumming DV, Latchman DS: Over-expression of heat shock protein 70 protects neuronal cells against both thermal and ischaemic stress but with different efficiencies. *Neurosci Lett* 1996, 206:45-48
20. Mailhos C, Howard MK, Latchman DS: Heat shock protects neuronal cells from programmed cell death by apoptosis. *Neuroscience* 1993, 55:621-627
21. Uney JB, Anderton BH, Thomas SM: Changes in heat shock protein 70 and ubiquitin mRNA levels in C1300 N2A mouse neuroblastoma cells following treatment with iron. *J Neurochem* 1993, 60:659-665

22. Wagstaff MJ, Collaco-Moraes Y, Smith J, de Belleruche JS, Coffin RS, Latchman DS: Protection of neuronal cells from apoptosis by Hsp27 delivered with a herpes simplex virus-based vector. *J Biol Chem* 1999, 274:5061–5069
23. Sodicoff M, Conger AD, Trepper P, Pratt NE: Short-term radioprotective effects of WR-2721 on the rat parotid glands. *Radiat Res* 1978, 75:317–326
24. Brizel DM, Wasserman TH, Henke M, Strnad V, Rudat V, Monnier A, Eschwege F, Zhang J, Russell L, Oster W, Sauer R: Phase III randomized trial of amifostine as a radioprotector in head and neck cancer. *J Clin Oncol* 2000, 18:3339–3345
25. Brizel DM, Overgaard J: Does amifostine have a role in chemoradiation treatment? *Lancet Oncol* 2003, 4:378–381
26. Schuchter L, Meropol NJ, Winer EP, Hensley ML, Somerfield MR: Amifostine and chemoradiation therapy: ASCO responds. *Lancet Oncol* 2003, 4:593
27. Park SH, Lee SJ, Chung HY, Kim TH, Cho CK, Yoo SY, Lee YS: Inducible heat-shock protein 70 is involved in the radioadaptive response. *Radiat Res* 2000, 153:318–326
28. Cho HN, Lee YJ, Cho CK, Lee SJ, Lee YS: Downregulation of ERK2 is essential for the inhibition of radiation-induced cell death in HSP25 overexpressed L929 cells. *Cell Death Differ* 2002, 9:448–456
29. Yi MJ, Park SH, Cho HN, Yong Chung H, Kim JI, Cho CK, Lee SJ, Lee YS: Heat-shock protein 25 (Hsp25) regulates manganese superoxide dismutase through activation of Nfkb (NF-kappaB). *Radiat Res* 2002, 158:641–649
30. Lee YJ, Cho HN, Jeoung DI, Soh JW, Cho CK, Bae S, Chung HY, Lee SJ, Lee YS: HSP25 overexpression attenuates oxidative stress-induced apoptosis: roles of ERK1/2 signaling and manganese superoxide dismutase. *Free Radic Biol Med* 2004, 36:429–444
31. Lee YJ, Lee DH, Cho CK, Bae S, Jhon GJ, Lee SJ, Soh JW, Lee YS: HSP25 inhibits protein kinase C delta-mediated cell death through direct interaction. *J Biol Chem* 2005, 280:18108–18119
32. Lee CT, Park KH, Yanagisawa K, Adachi Y, Ohm JE, Nadaf S, Dikov MM, Curiel DT, Carbone DP: Combination therapy with conditionally replicating adenovirus and replication defective adenovirus. *Cancer Res* 2004, 64:6660–6665
33. He TC, Zhou S, da Costa LT, Yu J, Kinzler KW, Vogelstein B: A simplified system for generating recombinant adenoviruses. *Proc Natl Acad Sci USA* 1998, 95:2509–2514
34. Edholm D, Molin M, Bajak E, Akusjarvi G: Adenovirus vector designed for expression of toxic proteins. *J Virol* 2001, 75:9579–9584
35. Becker TC, Noel RJ, Coats WS, Gomez-Foix AM, Alam T, Gerard RD, Newgard CB: Use of recombinant adenovirus for metabolic engineering of mammalian cells. *Methods Cell Biol* 1994, 43:161–189
36. Dreizen S, Brown LR, Handler S, Levy BM: Radiation-induced xerostomia in cancer patients. Effect on salivary and serum electrolytes. *Cancer* 1976, 38:273–278
37. Nagler RM, Baum BJ, Fox PC: Acute effects of X irradiation on the function of rat salivary glands. *Radiat Res* 1993, 136:42–47
38. Nagler RM: The enigmatic mechanism of irradiation-induced damage to the major salivary glands. *Oral Dis* 2002, 8:141–146
39. Cook DI, Van Lennep EW, Roberts ML, Young JA: Secretion by the major salivary glands. *Physiology of the Gastrointestinal Tract*, ed 3. Edited by LR Johnson. New York, Raven, 1994, pp 1061–1117
40. Winston DC, Hennigar RA, Spicer SS, Garrett JR, Schulte BA: Immunohistochemical localization of Na⁺, K⁺-ATPase in rodent and human salivary and lacrimal glands. *J Histochem Cytochem* 1988, 36:1139–1145
41. Ishida N, Hirai SI, Mita S: Immunolocalization of aquaporin homologs in mouse lacrimal glands. *Biochem Biophys Res Commun* 1997, 238:891–895
42. Matsuzaki T, Suzuki T, Koyama H, Tanaka S, Takata K: Aquaporin-5 (AQP5), a water channel protein, in the rat salivary and lacrimal glands: immunolocalization and effect of secretory stimulation. *Cell Tissue Res* 1999, 295:513–521
43. Poulsen JH, Bundgaard M: Quantitative estimation of the area of luminal and basolateral membranes of rat parotid acinar cells: some physiological applications. *Pflueg Arch Eur J Physiol* 1994, 429:240–244
44. Krane CM, Melvin JE, Nguyen HV, Richardson L, Towne JE, Doetschman T, Menon AG: Salivary acinar cells from aquaporin 5-deficient mice have decreased membrane water permeability and altered cell volume regulation. *J Biol Chem* 2001, 276:23413–23420
45. Nielsen S, King LS, Christensen BM, Agre P: Aquaporins in complex tissues. II. Subcellular distribution in respiratory and glandular tissues of rat. *Am J Physiol* 1997, 273:C1549–C1561
46. Ishikawa Y, Eguchi T, Skowronski MT, Ishida H: Acetylcholine acts on M3 muscarinic receptors and induces the translocation of aquaporin5 water channel via cytosolic Ca²⁺ elevation in rat parotid glands. *Biochem Biophys Res Commun* 1998, 245:835–840